Published in final edited form as:
Immunol Res. 2015 March ; 61(3): 177–186. doi:10.1007/s12026-015-8628-2.

Organ Distribution of Histones after Intravenous Infusion of FITC-Histones or after Sepsis

Fatemeh Fattahi[*], **Jamison J. Grailer**[*], **Lawrence Jajou**, **Firas S. Zetoune**, **Anuska V. Andjelkovic**, and **Peter A. Ward**[#]
Department of Pathology, University of Michigan Medical School, Ann Arbor, MI 48109 USA

Abstract

Histones appear in plasma during infectious or non-infectious sepsis and are associated with multiorgan injury. In the current studies, intravenous infusion of histones resulted in their localization in major organs. In vitro exposure of mouse macrophages to histones caused a buildup of histones on cell membranes followed by localization into cytosol and into the nucleus. After polymicrobial sepsis (cecal ligation and puncture, CLP), histones appeared in plasma as well as in a multiorgan pattern, peaking at 8 hr followed by decline. In lungs, histones and neutrophils appeared together, with evidence for formation of neutrophil extracellular traps (NETs), which represent an innate immune response to trap and kill bacteria and other infectious agents. In liver, there was intense NET formation, featuring linear patterns containing histones and strands of DNA. When neutrophils were activated in vitro with C5a or phorbol myristate acetate, NET formation ensued. While formation of NETs represents entrapment and killing of infectious agents, the simultaneous release from neutrophils of histones often results in tissue/organ damage.

Keywords

polymicrobial sepsis; C5a; C5aR1; C5aR2; NETs; organs

INTRODUCTION

Sepsis caused by infectious agents (bacteria, viruses, fungi) or after “sterile sepsis” (such as polytrauma or hemorrhagic shock [1, 2]) is associated with the appearance in plasma of histones which are derived from nucleosomes containing histones that are tightly bound to coils of DNA, being released as the DNA unravels [3, 4]. Histones are known to be cell-damaging for both parenchymal cells and vascular endothelial cells [5–8] and are highly prothrombotic [5, 9–13]. Their presence in plasma has been associated with endothelial cell dysfunction [7, 8, 12–14], loss of the blood/gas barrier in lung, and damage in major organs [5–9, 15]. It is also known that a protective mechanism is hydrolysis and inactivation of histones by activated protein C [6–8, 15]. Previous studies have indicated that the

[#]Corresponding Author: Godfrey D. Stobbe Professor of Pathology, University of Michigan Medical School, Department of Pathology, 7520 MSRB I, 1301 Catherine Rd., Ann Arbor, MI 48109-5602, Tel. 734-647-2921, Fax 734-764-4308, pward@umich.edu.
[*]Equally Contributing Authors

The authors declare no commercial or financial conflicts of interests.

appearance of histones during infectious [7, 8, 15–17] or sterile [5, 12, 18–23] sepsis can be linked to organ failure and lethality.

Histones function as “danger associated molecular patterns” (DAMPs), interacting with cells of the innate immune system, including neutrophils (PMNs) and macrophages and other cell types, triggering production of cytokines and chemokines, which provide a defensive shield designed to contain infectious agent(s). Based on limited evidence, it appears that histones interact with TLR2 and TLR4 [6, 11, 18, 24] and perhaps NLRs [21, 22, 25], resulting in activation of these cells to release proinflammatory products. Obviously, such responses may be protective if the amount of histones present is limited, but excessive histone release can result in organ and tissue damage linked to an excessive inflammatory response that exacerbates tissue injury, along with prothrombotic outcomes.

An important source of histones in septic shock appears to be PMNs which, when activated by the complement anaphylatoxin, C5a, bacterial lipopolysaccharide (LPS) or phorbol myristate acetate (PMA), form NETs. NETs are composed of strands of DNA and contain histones as well as products from neutrophil granules including myeloperoxidase (MPO). It is now clear that NETs represent a potent innate immune response that restrains bacteria, viruses, and fungi, leading to their inactivation or destruction. NETs also seem to be an important source of histones appearing in plasma during sepsis and in lung during development of acute lung injury (ALI) [5–7, 9, 14, 16, 26, 27].

In our recent studies, acute lung injury (ALI) in mice was triggered by lung deposition of any of the following phlogistic agonists: lipopolysaccharide, IgG immune complexes (IgGIC), or the powerful complement-derived anaphylatoxin, C5a [20, 21, 23]. Lung deposition of these powerful agonists is associated in the case of IgGIC or LPS with triggering of the complement system, resulting in generation of C5a. C5a interacts with its receptors (C5aR1, C5aR2), causing activation of lung PMNs and macrophages, which leads to a surge in lung of proinflammatory cytokines and chemokines [20, 21, 23, 28]. Accompanying these responses is C5a-induced activation of PMNs, leading to C5a receptor-dependent activation and formation of NETs, followed by release of histones [20, 21]. Besides their intrinsic powerful phlogistic properties, histones can activate the NLRP3 inflammasome, resulting in release from phagocytic cells of IL-1β and IL-18, which further intensify the inflammatory response [21].

In the current report, we focus on the ability of plasma histones occurring after CLP or following infusion of FITC-histones to localize in various organs, especially lung and liver, both of which are known to be injured in the course of infectious [7, 8, 15–17] or non-infectious (“sterile”) [5, 12, 18–23] sepsis. We demonstrate in vitro that activated PMNs from NETs and that histones attach to macrophage surfaces and become internalized. After CLP, there is extensive presence of histones and NETs in lungs and liver. The appearance of histones released from NETs results in intensified organ damage.

MATERIALS AND METHODS

Animals

All procedures were performed within the U.S. National Institutes of Health guidelines and were approved by the University of Michigan Committee on the Use and Care of Animals. Male C57BL/6 wild type mice were purchased from the Jackson Laboratories (Bar Harbor, ME). All animals were housed under specific pathogen-free conditions with free access to food and water.

Reagents

Mixed calf thymus histones (purified, Type II-A), LPS (E. coli o111:B4), and phorbol 12-myristate 13-acetate (PMA), were purchased from Sigma (St. Louis, MO), and recombinant mouse C5a from R&D Systems (Minneapolis, MN). Mixed histone (from calf thymus) preparations were used in experiments unless otherwise indicated. H1 histone from purified calf thymus (Roche, Indianapolis, IN) was also used in this study. Histone stocks were dissolved in PBS, pH 7.4, and stored at −80°C until use. Histone preparations were essentially endotoxin-free [20]. Anti-histone H2A/H4 antibody (clone BWA3 [29]) was purified from ascites by protein A/G chromatography.

In vitro assays

Mouse peritoneal macrophages (PEMs) were elicited by intra peritoneal (i.p.) injection of 1.5 ml of 2.4% thioglycollate (Life Technologies, Grand Island, NY). Macrophages were harvested 4 days later by i.p. instillation and retraction of 8 ml sterile PBS.

Mouse PMNs were harvested from bone marrow by flushing femurs with Hanks' balanced salt solution; HBSS (Life Technologies, Grand Island, NY). Erythrocytes were lysed in hypotonic buffer. Cells were washed in PBS and layered on Histopaque 1077 (Sigma-Aldrich, St. Louis, MO) for density gradient centrifugation (500 × g, 30 min, 4°C). The pellet (PMNs) was washed with PBS prior to downstream applications. PMN purity was 85 ± 2% as determined by Wright-stained cytospin preparations.

Cecal ligation and puncture (CLP)

Mid-grade CLP (~50% survival after 7 days) was used for this study, as described previously [30]. Sham animals underwent the same procedure without ligation and puncture. The animals were euthanized at times indicated after CLP. All animals (sham and CLP) received fluid resuscitation (1.5 ml lactated Ringers, given subcutaneously into the nuchal region).

Blood collection

Blood anticoagulated with acid-citrate-dextrose (ACD) was collected by cardiac puncture 8 hr after the induction of CLP. Plasma was evaluated for the histone levels by ELISAs (Roche, Indianapolis, IN).

Confocal Imaging

For confocal imaging of cells, PMNs and macrophages were plated on sterile 22 mm coverslips in 6-well plates for 1–2 hr to let cells adhere as best as possible. Then the activator (C5a or PMA) was added and incubated for 90 minutes at 37°C. Immunofluorescence staining followed. For studying uptake of histones, cells were incubated with FITC-conjugated histones or AF488-H1 up to 30 min at 37°C.

The following antibodies were used for immunofluorescent labeling: anti-mouse IgG-TRITC (Jackson Immunoresearch, West Grove, PA), anti-mouse IgG-AlexaFluor488 (Jackson Immunoresearch, West Grove, PA), and anti-mouse Ly6G-AlexaFluor647 (eBioscience, San Diego, CA). Slides were mounted with ProLong Gold anti-fade reagent containing DAPI (Life Technologies Grand Island, NY). Digital monochromatic images were acquired on a Nikon A-1 confocal system with Nikon Elements software.

FITC-labeled Histones

37.5 μg FITC (Sigma-Aldrich, St. Louis, MO) was conjugated to 1 mg of mixed calf thymus histones according to established procedures [31]. For in vivo experiments 45 mg/kg bodyweight histones were injected i.v. and FITC in different organs homogenates were analyzed by fluorescence plate reader (excitation 485, emission 535).

Determination of tissue histone content

For determination of histone content, tissues were mechanically homogenized in PBS containing protease inhibitors (Roche, Indianapolis, IN). Total protein estimations were determined by the BCA assay (Sigma-Aldrich, St. Louis, MO). Histone content was then measured by ELISA (Roche). Purified mixed calf thymus histones were used to generate standard curves as described [20].

Statistical analysis

Data were expressed as mean ± SEM. Data was analyzed using GraphPad Prism 6 graphing and statistical analysis software (GraphPad Inc., La Jolla, CA). Significant differences between sample means were determined using the Student’s t test (two-tailed). A p value <0.05 was considered to be significant.

RESULTS

Histone Binding to Macrophages and Internalization of FITC-histones (Figure 1)

A histone mixture (50 μg/ml) was labeled with FITC and then incubated at 37°C with mouse peritoneal exudate macrophages (PEMs) for times varying from 1 min to 30 min. Cells were then assessed by fluorescent microscopy. DAPI stain was used to define nuclei within PEMs. The results are shown in Figure 1. With the histone mix, no PEM staining for histones was detected at 1 min. By 5 min, surface staining began to appear. At 15 min, histones were present on the cell surfaces as well as in the cytosol and nucleus of PEMs. By 30 min, there was extensive fluorescence indicative of histones on the cell surfaces, in the cytosol and in the nucleus. DAPI staining clearly also showed colocalization of histones within the nucleus. When similar studies were done with AF488-H1 (lowest frames) (Figure

1), some surface staining occurred at 1 min, progressing by 5 and 15 min with surface and cytosolic staining. By 30 min, intense cytosolic and nuclear staining was apparent.

Organ Content of Histones after Infusion of FITC-histones or after CLP (Figure 2)

Since in polymicrobial sepsis histones are known to appear in the plasma 6 to 30 hr after CLP [7, 18], we decided to determine the extent to which histones appear in various organs. Appearance of histones in various organs could perhaps be linked to subsequent development of multiorgan failure. In Figure 2A, the FITC-histone mix (45 μg/kg body weight) was infused intravenously (via tail vein). 8 hr later organs were obtained, perfused with PBS to remove blood and then subjected to homogenization. For each bar in Figure 2, n ≥ 5 individual mice. The homogenates were then examined for FITC-histone content. Results were expressed as ng/mg protein, as shown in Figure 2A. The greatest histone content appeared in lung (nearly 6,000 ng/mg protein). Content of histones in spleen was the second highest level (nearly 800 ng/mg protein, followed by kidney, liver, heart, and brain). Plasma content of FITC-histones is also shown. That histone content was highest in lung may have been due either to the extensive surface area of the pulmonary capillary surface or because the lung was the first organ to encounter the histones which were infused intravenously. It is known that histones can bind to endothelial cells [5, 7].

In Figure 2B, we assessed histone content (using ELISA which detects all histones, [20]) in a variety of organs obtained from mice 8 hr after CLP. The rank order of histone content in organ homogenates was spleen > liver > lung, followed by much lower histone content in kidney, heart and brain. This pattern of organ content of histones may reflect the reticuloendothelial system which is prominently present in spleen, liver and lung. Alternatively, it may also be that, during CLP-induced sepsis, there is synthesis of histones in the various organs described in Figure 2, although this has not been proven.

Time Course for Appearance of Histones in Various Organs after CLP (Figure 3)

We assessed (by ELISA) the appearance of histones in organ homogenates as a function of time after CLP. Histone presence was expressed as μg/mg protein in the homogenates. Six different organs were examined at times 0, 4, 8, 18 and 30 hr after CLP (Figure 3). For all data points, n=4–7 mice for each time point. Similar to the data in Figure 2B, the spleen was the most enriched in histones, which peaked 8 hr after CLP, declining thereafter, and leveling off at approximately 100 μg/mg protein (Figure 3A) 20–30 hr after CLP. A rather similar pattern, but quantitatively at much lower levels, was found in lung (Figure 3B). In the liver, the histone peak occurred 8 hr after CLP and declined thereafter to baseline levels (Figure 3C). In the kidney (frame D), there was a barely perceptible increase in histone content at 8 hr (not statistically significant), with decline to baseline thereafter. In the heart, a peak of histone presence occurred 4 hr after CLP (frame E), followed by a decline and then a small incline. It should be noted that all histone levels were quite low when compared to those in the spleen. In the brain, statistically there were no significant changes in histone levels after CLP.

These data suggest that histone appearance after CLP could be due to binding of histones in plasma to endothelial cells, or related to internalization of plasma histones into organs

(perhaps similar to the phenomena described in Figure 1), or uptake by the reticuloendothelial system in various organs (spleen, liver, lungs). Alternatively, CLP may trigger local synthesis of histones in various organs. Limitations in available technology do not permit the resolution of these questions.

Appearance of Histones in Lung after CLP (Figure 4)

In Figure 4, frozen sections of lung 8 hr after CLP were obtained and assessed for content of PMNs (Ly6G epitope), histones, DAPI staining, together with merged images. In the top set of frames, sections from normal (ctrl) lungs showed little or no evidence of PMNs (red staining indicating the Ly6G epitope) or histone presence (green staining). As expected, DAPI staining (including that in the merge image) showed diffuse blue staining indicative of DNA in nuclei of the alveolar and capillary networks. In striking contrast, lung frozen sections 8 hr after CLP revealed red staining in alveolar and capillary walls indicating the Ly6G epitope for PMNs. In this and subsequent figures, scale bars indicate magnifications of the images. The diffuse lung staining (red) is consistent with the plethora of PMNs known to accumulate in lung capillaries after CLP [28]. Histone staining (green) was also evident in lung sections after CLP, present in both a granular and a linear pattern (histone frame). DAPI staining in the sections after CLP showed diffuse staining including linear patterns in alveolar and capillary walls. The merge image indicated histone presence and early evidence of linear staining, suggesting the presence of NETs. The frames revealed extensive histone presence in lung, some being associated with blue staining nuclei, while others were not related to nuclear staining (lowest right frame, arrowheads). The reference to the histone pattern of staining being both granular and linear suggests that histone appearance in lung after CLP may be the result of early formation of neutrophil extracellular traps (NETs) following the activation of PMNs with C5a generated in the early phases of sepsis [20, 32]. Indeed, one of our recent publications suggests that acute lung injury induced by airway instillation of LPS results in the appearance of histones, formation of which was both complement (C5a) and PMN-dependent [20].

In Vitro and In Vivo Formation of NETs and Histone Presence (Figure 5)

In Figure 5, purified bone marrow PMNs (A, B) were exposed in vitro to PMA (50 ng/ml) or rmC5a (1 μg/ml) for 90 min at 37°C and then analyzed by fluorescence microscopy for the presence of histones (red color), DAPI staining (blue color), and the merge images. In frame A, histone presence occurred in long strand-like structures, the merge images (pink and white) at the end of the strands representing the coalescence of the red and blue stains in PMNs. In frame B, PMNs showed extensions that appeared to represent early NET formation with histone presence (red), with DAPI staining of nuclei, while the merge images (pink, white) appeared to represent the combination of red and blue fluorescence. In frame C, frozen sections of lung 8 hr after CLP showed extensive presence of the PMN epitope (Ly6G) in alveolar and capillary walls (red color), associated with the green staining for histones. DAPI stains appeared to be predominantly confined to nuclei, although in some areas early linear staining seemed to be occurring. The merge image indicated pink and white staining for copresence of the PMN epitope and histones, with areas of discrete histone (green) staining, together with areas of DAPI staining which may represent intact nuclei as well as early NET formation.

Appearance of Histones and NETs in Liver after CLP (Figure 6)

We also focused on the appearance of histones in liver 8 hr after CLP. The data are shown in Figure 6. In normal (ctrl) liver, we found limited histone presence as indicated by scattered faint green granular fluorescence. The DAPI stain indicated the diffuse presence of nuclear staining. The merge imaged revealed predominantly granular staining. In the 8 hr CLP liver, it was clear that intense green staining for histone was present, both in a granular and linear pattern as found in histones and DAPI as well as in the merge stains. The merge images clearly showed linear staining, which would be consistent with the presence of NETs. At the highest magnification (lowest frames), the histone staining (green) was strikingly linear, as was the DAPI (blue) staining which likely represents DNA and nuclear histones. The merge image showed that the linear configurations contained both histones and DNA (green and blue staining). Thus, CLP at 8 hr caused extensive NET formation in liver.

DISCUSSION

Based on increasing evidence that histone presence occurs both in infectious [7, 8, 15–17] and in noninfectious (sterile) sepsis [5, 12, 18–23], we decided to assess histone presence in plasma and in organs either after infusion into Wt mice of FITC-histones or after CLP. Several groups have found substantial histone presence in plasma after blunt trauma, CLP or after chemically induced acute liver injury [5, 7, 18] and have shown by ELISA or by limited Western blot analysis substantial (20–40 μg/ml) amounts of histones in plasma after CLP or ALI [20, 21]. The origin of such histones may be formation of NETs in PMNs caused by the complement activation product, C5a which interacts with its two receptors (C5aR1, C5aR2) to propagate the inflammatory response. The source of plasma histones may be release of histones from nucleosomes in which histones are very tightly packed. As the sepsis process proceeds, peptidyl arginine deiminase 4 (PAD4) in PMNs is activated and converts arginine in histone protein cores (involving H2A, H3 and H4) to citrulline via a deamination process [33]. It has been suggested that this process may cause the uncoiling of DNA, leading to release of histones [34]. Histones are known to be damaging to various cell types (endothelial cells and alveolar wall epithelial cells) in lung [5, 12], to be highly phlogistic, and to be intensely thrombogenic [5, 9–13]. Infusion of relatively high concentrations of histones causes lethality in mice [7, 10, 18]. Interestingly, activated protein C, which is a naturally occurring antithrombotic factor, has the ability to degrade histones [6–8, 13, 15]. In the setting of either infectious or sterile sepsis, histones appear to play important roles in harmful outcomes. This is based on direct evidence of protection in CLP mice treated with a histone neutralizing antibody and lethal effects of infused histones [7, 13]. The mAb neutralized both H2A and H4 [7]. In addition, in the setting of ALI in mice, in which histones have been detected in BALF, this mAb greatly attenuated the intensity of albumin leak into lungs, reduced the cytokine/chemokine surge, and greatly attenuated the histopathological features of ALI [20, 21].

The finding of histones in various organs after CLP (Figures 2, 3) and in lungs and liver (Figures 4–6) as determined by immunofluorescence raises the question about whether the histones found in lungs and liver are derived from the plasma histones or are generated locally following CLP, or due to a combined mechanism. Currently, it is difficult to answer

this question because of the lack of reliable agents to quantitate specific histones. If individual content of histones in liver and lung after CLP were to show differences from the individual histones present in plasma after CLP, such evidence might suggest the local synthesis of histones.

Acknowledgments

This work was supported by grants from the National Institutes of Health, GM-29507 and GM-61656 (PAW). The authors are responsible for the scientific content of this publication. We also acknowledge the expert assistance of Sue Scott and Melissa Rennells with the manuscript preparation.

References

1. Ward PA. An endogenous factor mediates shock-induced injury. Nat Med. 2013; 19(11):1368–9.10.1038/nm.3387 [PubMed: 24202382]
2. Tang D, Kang R, Coyne CB, Zeh HJ, Lotze MT. PAMPs and DAMPs: signal 0s that spur autophagy and immunity. Immunol Rev. 2012; 249(1):158–75.10.1111/j.1600-065X.2012.01146.x [PubMed: 22889221]
3. Richmond TJ, Davey CA. The structure of DNA in the nucleosome core. Nature. 2003; 423(6936): 145–50.10.1038/nature01595 [PubMed: 12736678]
4. Luger K, Mader AW, Richmond RK, Sargent DF, Richmond TJ. Crystal structure of the nucleosome core particle at 2.8 A resolution. Nature. 1997; 389(6648):251–60.10.1038/38444 [PubMed: 9305837]
5. Abrams ST, Zhang N, Manson J, Liu T, Dart C, Baluwa F, et al. Circulating histones are mediators of trauma-associated lung injury. Am J Respir Crit Care Med. 2013; 187(2):160–9.10.1164/rccm.201206-1037OC [PubMed: 23220920]
6. Allam R, Scherbaum CR, Darisipudi MN, Mulay SR, Hagele H, Lichtnekert J, et al. Histones from dying renal cells aggravate kidney injury via TLR2 and TLR4. J Am Soc Nephrol. 2012; 23(8): 1375–88.10.1681/ASN.2011111077 [PubMed: 22677551]
7. Xu J, Zhang X, Pelayo R, Monestier M, Ammollo CT, Semeraro F, et al. Extracellular histones are major mediators of death in sepsis. Nat Med. 2009; 15(11):1318–21.10.1038/nm.2053 [PubMed: 19855397]
8. Gillrie MR, Lee K, Gowda DC, Davis SP, Monestier M, Cui L, et al. Plasmodium falciparum histones induce endothelial proinflammatory response and barrier dysfunction. Am J Pathol. 2012; 180(3):1028–39.10.1016/j.ajpath.2011.11.037 [PubMed: 22260922]
9. Allam R, Kumar SV, Darisipudi MN, Anders HJ. Extracellular histones in tissue injury and inflammation. J Mol Med (Berl). 2014; 92(5):465–72.10.1007/s00109-014-1148-z [PubMed: 24706102]
10. Chen R, Kang R, Fan XG, Tang D. Release and activity of histone in diseases. Cell Death Dis. 2014; 5:e1370.10.1038/cddis.2014.337 [PubMed: 25118930]
11. Semeraro F, Ammollo CT, Morrissey JH, Dale GL, Friese P, Esmon NL, et al. Extracellular histones promote thrombin generation through platelet-dependent mechanisms: involvement of platelet TLR2 and TLR4. Blood. 2011; 118(7):1952–61.10.1182/blood-2011-03-343061 [PubMed: 21673343]
12. Caudrillier A, Kessenbrock K, Gilliss BM, Nguyen JX, Marques MB, Monestier M, et al. Platelets induce neutrophil extracellular traps in transfusion-related acute lung injury. J Clin Invest. 2012; 122(7):2661–71.10.1172/JCI61303 [PubMed: 22684106]
13. Nakahara M, Ito T, Kawahara K, Yamamoto M, Nagasato T, Shrestha B, et al. Recombinant thrombomodulin protects mice against histone-induced lethal thromboembolism. PLoS One. 2013; 8(9):e75961.10.1371/journal.pone.0075961 [PubMed: 24098750]
14. Saffarzadeh M, Juenemann C, Queisser MA, Lochnit G, Barreto G, Galuska SP, et al. Neutrophil extracellular traps directly induce epithelial and endothelial cell death: a predominant role of histones. PLoS One. 2012; 7(2):e32366.10.1371/journal.pone.0032366 [PubMed: 22389696]

15. Ekaney ML, Otto GP, Sossdorf M, Sponholz C, Boehringer M, Loesche W, et al. Impact of plasma histones in human sepsis and their contribution to cellular injury and inflammation. Crit Care. 2014; 18(5):543.10.1186/s13054-014-0543-8 [PubMed: 25260379]
16. Hashiba M, Huq A, Tomino A, Hirakawa A, Hattori T, Miyabe H, et al. Neutrophil extracellular traps in patients with sepsis. J Surg Res. 201410.1016/j.jss.2014.09.033
17. Luo L, Zhang S, Wang Y, Rahman M, Syk I, Zhang E, et al. Proinflammatory role of neutrophil extracellular traps in abdominal sepsis. Am J Physiol Lung Cell Mol Physiol. 2014; 307(7):L586–96.10.1152/ajplung.00365.2013 [PubMed: 25085626]
18. Xu J, Zhang X, Monestier M, Esmon NL, Esmon CT. Extracellular histones are mediators of death through TLR2 and TLR4 in mouse fatal liver injury. J Immunol. 2011; 187(5):2626–31.10.4049/jimmunol.1003930 [PubMed: 21784973]
19. Huang H, Evankovich J, Yan W, Nace G, Zhang L, Ross M, et al. Endogenous histones function as alarmins in sterile inflammatory liver injury through Toll-like receptor 9 in mice. Hepatology. 2011; 54(3):999–1008.10.1002/hep.24501 [PubMed: 21721026]
20. Bosmann M, Grailer JJ, Ruemmler R, Russkamp NF, Zetoune FS, Sarma JV, et al. Extracellular histones are essential effectors of C5aR- and C5L2-mediated tissue damage and inflammation in acute lung injury. FASEB J. 2013; 27(12):5010–21.10.1096/fj.13-236380 [PubMed: 23982144]
21. Grailer JJ, Canning BA, Kalbitz M, Haggadone MD, Dhond RM, Andjelkovic AV, et al. Critical role for the NLRP3 inflammasome during acute lung injury. J Immunol. 2014; 192(12):5974–83.10.4049/jimmunol.1400368 [PubMed: 24795455]
22. Huang H, Chen HW, Evankovich J, Yan W, Rosborough BR, Nace GW, et al. Histones activate the NLRP3 inflammasome in Kupffer cells during sterile inflammatory liver injury. J Immunol. 2013; 191(5):2665–79.10.4049/jimmunol.1202733 [PubMed: 23904166]
23. Bosmann M, Grailer JJ, Zhu K, Matthay MA, Sarma JV, Zetoune FS, et al. Anti-inflammatory effects of beta2 adrenergic receptor agonists in experimental acute lung injury. FASEB J. 2012; 26(5):2137–44.10.1096/fj.11-201640 [PubMed: 22318967]
24. Darwiche SS, Ruan X, Hoffman MK, Zettel KR, Tracy AP, Schroeder LM, et al. Selective roles for toll-like receptors 2, 4, and 9 in systemic inflammation and immune dysfunction following peripheral tissue injury. J Trauma Acute Care Surg. 2013; 74(6):1454–61.10.1097/TA.0b013e3182905ed2 [PubMed: 23694872]
25. Allam R, Darisipudi MN, Tschopp J, Anders HJ. Histones trigger sterile inflammation by activating the NLRP3 inflammasome. Eur J Immunol. 2013; 43(12):3336–42.10.1002/eji.201243224 [PubMed: 23964013]
26. McDonald B, Urrutia R, Yipp BG, Jenne CN, Kubes P. Intravascular neutrophil extracellular traps capture bacteria from the bloodstream during sepsis. Cell Host Microbe. 2012; 12(3):324–33.10.1016/j.chom.2012.06.011 [PubMed: 22980329]
27. Tanaka K, Koike Y, Shimura T, Okigami M, Ide S, Toiyama Y, et al. In vivo characterization of neutrophil extracellular traps in various organs of a murine sepsis model. PLoS One. 2014; 9(11):e111888.10.1371/journal.pone.0111888 [PubMed: 25372699]
28. Grailer JJ, Kalbitz M, Zetoune FS, Ward PA. Persistent neutrophil dysfunction and suppression of acute lung injury in mice following cecal ligation and puncture sepsis. J Innate Immun. 2014; 6(5):695–705.10.1159/000362554 [PubMed: 24861731]
29. Monestier M, Fasy TM, Losman MJ, Novick KE, Muller S. Structure and binding properties of monoclonal antibodies to core histones from autoimmune mice. Mol Immunol. 1993; 30(12):1069–75. [PubMed: 8366857]
30. Rittirsch D, Huber-Lang MS, Flierl MA, Ward PA. Immunodesign of experimental sepsis by cecal ligation and puncture. Nat Protoc. 2009; 4(1):31–6.10.1038/nprot.2008.214 [PubMed: 19131954]
31. Yipp BG, Petri B, Salina D, Jenne CN, Scott BN, Zbytnuik LD, et al. Infection-induced NETosis is a dynamic process involving neutrophil multitasking in vivo. Nat Med. 2012; 18(9):1386–93.10.1038/nm.2847 [PubMed: 22922410]
32. Bosmann M, Ward PA. Role of C3, C5 and anaphylatoxin receptors in acute lung injury and in sepsis. Adv Exp Med Biol. 2012; 946:147–59.10.1007/978-1-4614-0106-3_9 [PubMed: 21948367]

33. Ham A, Rabadi M, Kim M, Brown KM, Ma Z, D'Agati V, et al. Peptidyl arginine deiminase-4 activation exacerbates kidney ischemia-reperfusion injury. Am J Physiol Renal Physiol. 2014; 307(9):F1052–62.10.1152/ajprenal.00243.2014 [PubMed: 25164081]

34. Martinod K, Demers M, Fuchs TA, Wong SL, Brill A, Gallant M, et al. Neutrophil histone modification by peptidylarginine deiminase 4 is critical for deep vein thrombosis in mice. Proc Natl Acad Sci U S A. 2013; 110(21):8674–9.10.1073/pnas.1301059110 [PubMed: 23650392]

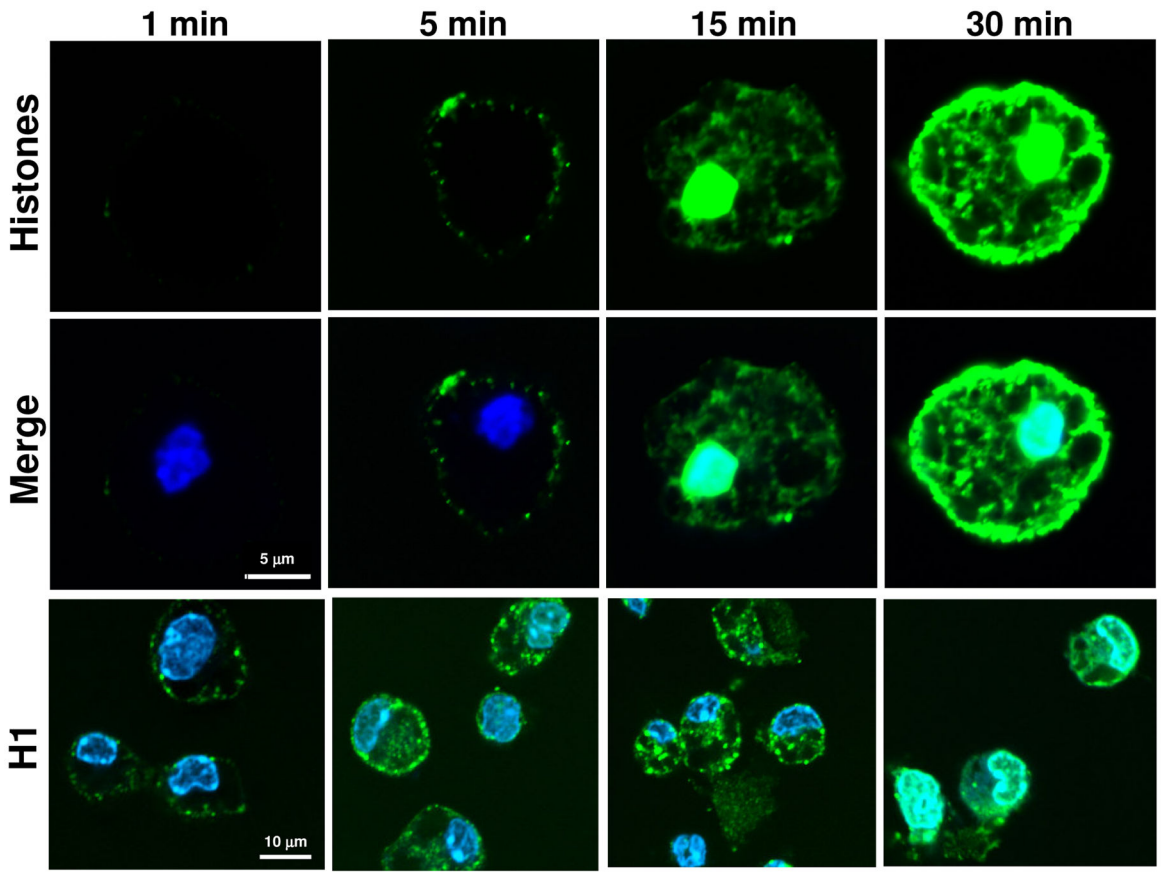

Figure 1. Uptake of FITC-histones (mix or H1) by mouse peritoneal macrophages (PEMs)

Mouse peritoneal macrophages were incubated with an FITC-histone mix or with AF488-H1 (50 μg/ml at 37°C for the times indicated) and then evaluated by fluorescence microscopy. Upper frames: Uptake of FITC-histones over 1–30 min indicated spotty surface of histone binding to PEMs after 5 min incubation, followed at 15 min by both surface binding and uptake of histones into the cytosol and nucleus. At 30 min, there was extensive surface, cytosolic and nuclear presence of histones. Middle frames: Uptake of FITC-histones, using DAPI stained macrophages in which the nucleus was blue staining. The 15 and 30 min frames indicated that histones also accumulated in the nucleus. Lower frames: Macrophages were exposed to AF488-labeled H1, resulting in features similar to those obtained with the FITC mix, indicating H1 localization occurring on cell surfaces, in the cytosol, and in nuclei. Data are representative of three separate and independent experiments.

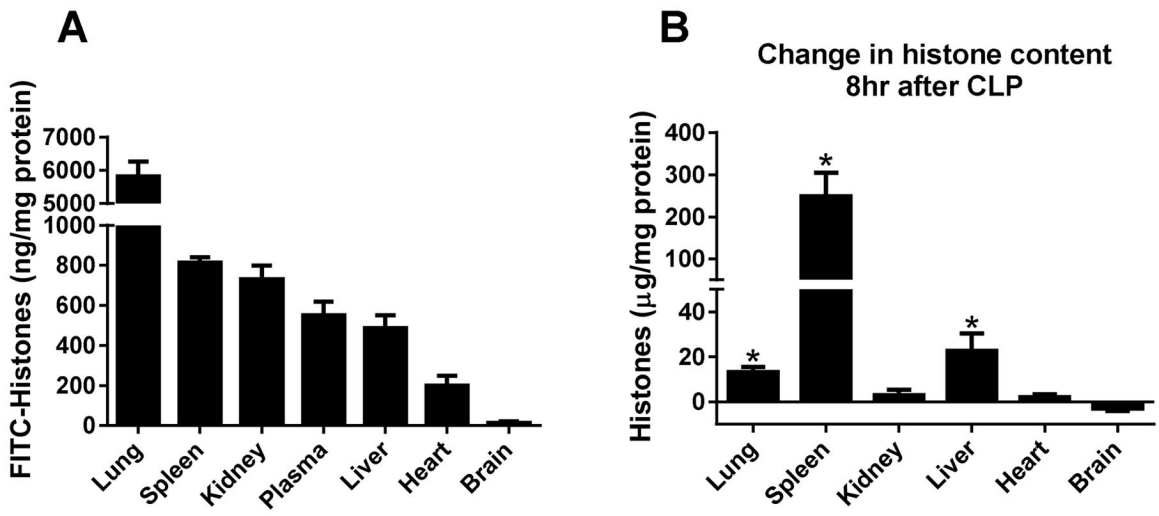

Figure 2. Organ Uptake of Histones after I.V. Infusion of FITC-histones or 8 hr after CLP

In frame A, FITC-histones (45 mg/kg body weight) were infused i.v. (tail vein) into young adult (8–9 weeks) male Wt C57BL/6 mice and 8 hr later organs were perfused with PBS to remove blood and then homogenized. The quantity of FITC-histones was calculated in organs and expressed as ng histones/mg protein. Results are shown in descending order of histone amounts computed. For each bar, n ≥ 5 mice. In frame B, mice were subjected to CLP. 8 hr later, organs were isolated, perfused with PBS and then homogenates were obtained and histone presence quantitated by ELISA. Histone content was expressed as μg/mg protein in the homogenates. For each bar, n ≥ 5 mice.

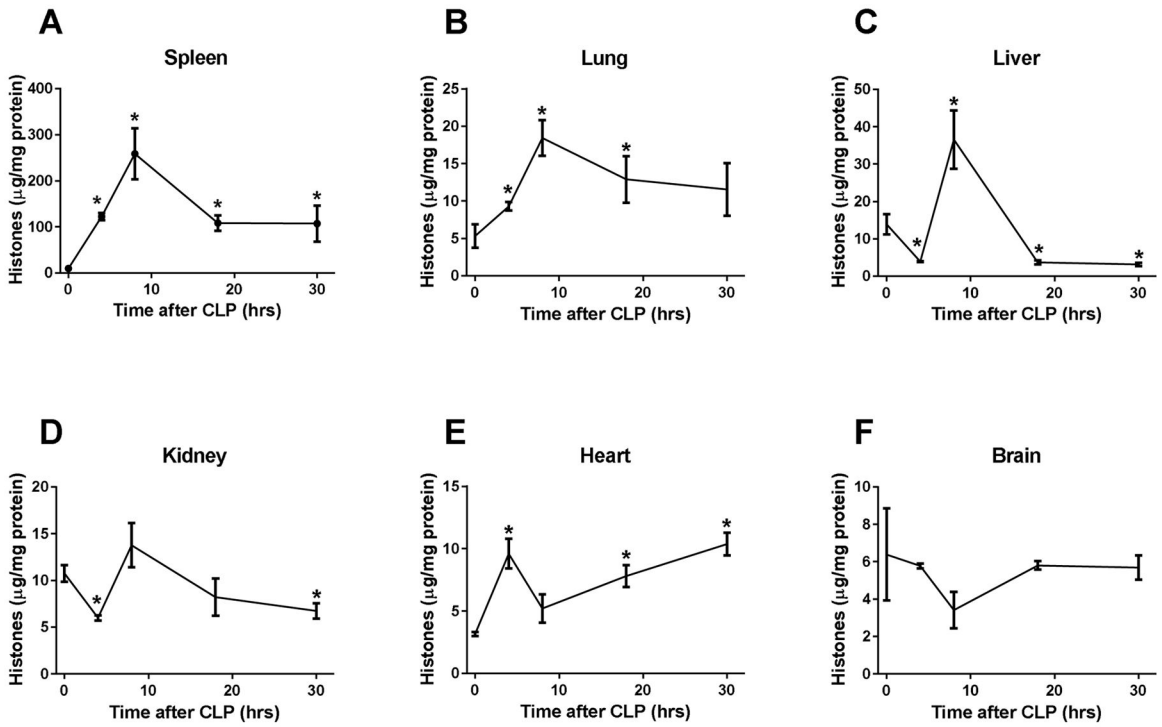

Figure 3. Appearance of Histones in Organs at Different Time Points after CLP

For these experiments, organs were obtained at times 0, 4, 8, 18 and 30 hr after CLP. Organs were then perfused with PBS to remove blood, and homogenates were obtained to quantitate histone content, which was expressed as μg/mg protein based on ELISA analysis.. The spleen contained the highest amounts of histone, followed by liver and other organs. In general, histone content in organs peaked 8 hr after CLP, followed by a decline. For each data point, $n \geq 5$ mice.

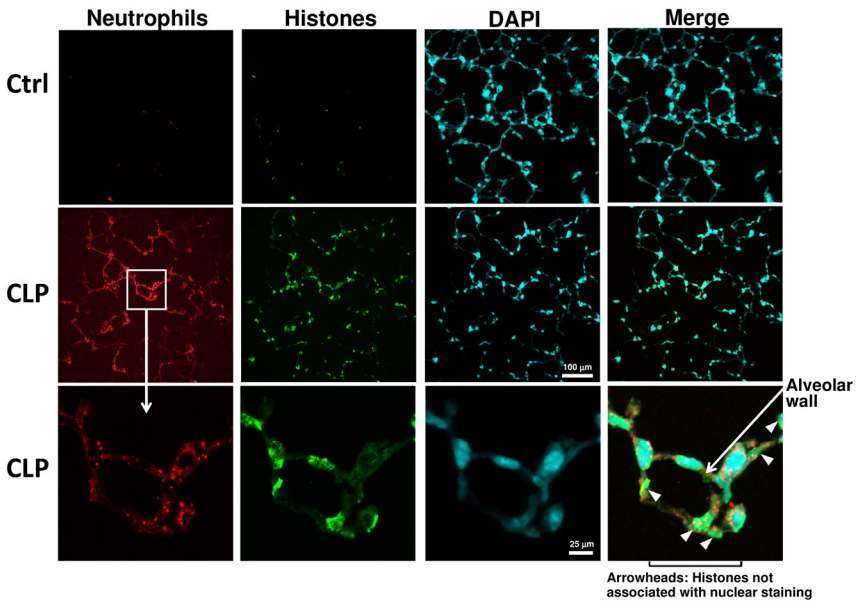

Figure 4. Content of Histones in Lungs as Assessed by Frozen Sections before and 8 hr after CLP

Upper frames: Little if any staining for PMNs (red) or histones (green) was present in control lungs. DAPI staining (blue) was present in nuclei in alveolar walls and capillaries and was little changed in the merge image. Middle frames: 8 hr after CLP (lower magnification), PMN presence (Ly6G epitope, red) appeared in alveolar and capillary walls. Histone presence (green) was defined by both a granular and developing linear pattern. The merge confirmed this pattern, showing both blue and green granular and linear staining. Lower frames: At a higher magnification, PMN epitopes (red staining) were present both in alveolar and capillary walls, while histone staining (green) was found in similar locations. The merge image showed histone presence both in nuclei and in cytoplasmic (arrowheads) areas along with red staining indicating the Ly6G epitope for PMNs.

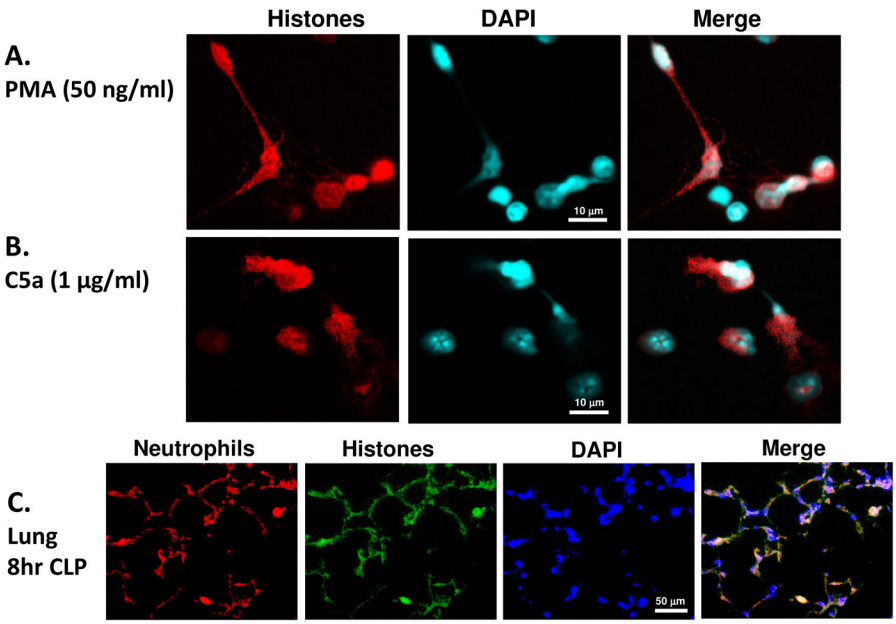

Figure 5. NET Formation in PMNs Exposed to PMA or C5a and in lung 8 hr after CLP

In frames A and B, purified bone marrow PMNs were exposed to PMA (50 ng/ml) or to rmC5a (1 μg/ml) for 90 min at 37°C. The cells were then fixed with 1.5% formaldehyde for 10 min at room temp, incubated with BWA3 Ab to detect H2A/H4 followed by a donkey fluorescence antibody. Red stain represents histones while blue color DAPI stained nuclei. Exposure of PMN to PMA or C5a caused extensions of histones (red) between cells, representing histone positive NETs, while merger stains created white fluorescence indicated pink and white co-fluorescence of red and blue fluorescence. C5a induced prolongation of PMNs which were histone-positive, apparently representing early NET formation. In frame C, lung frozen sections 8 hr after CLP demonstrated PMNs (red fluorescence), histones (green fluorescence) and DAPI stains. The merge image indicated white and pink areas (due to colocalization of red and green fluorescence) as well as DAPI positive regions.

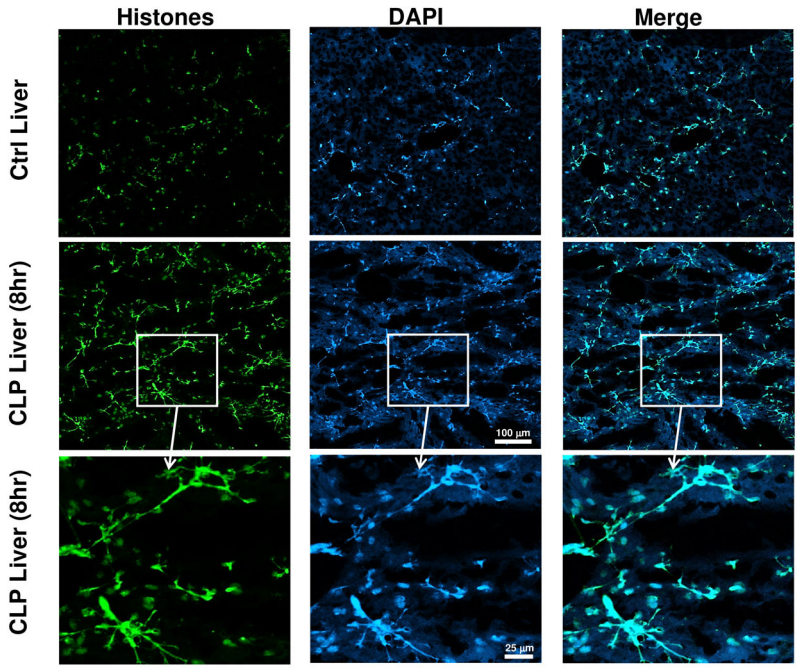

Figure 6. Liver Content of Histones in Frozen Sections before and 8 hr after CLP

Upper frames represent control liver sections stained for histones (green stain), DAPI (blue stain) and the merge image. Faint histone presence was found in ctrl liver sections containing DAPI positive staining nuclei. The merge image was rather faint but showed some evidence of granular and linear staining. Middle frames revealed both accentuated granular and a linear patterns for histones and DNA. The merge image confirmed a strong linear pattern for histones (lower magnification). Lower frames (at higher magnification) showed a striking linear pattern for histones, while DAPI showed a similar image, and the merge confirmed that histones (green) and DNA (blue) were present in the linear areas, indicating the presence of NETs.